Formation of nitrogen- and sulfur-containing light-absorbing compounds accelerated by evaporation of water from secondary organic aerosols

Tran B. Nguyen,[1] Paula B. Lee,[1] Katelyn M. Updyke,[1] David L. Bones,[1] Julia Laskin,[2] Alexander Laskin,[3] and Sergey A. Nizkorodov[1]

Received 29 September 2011; revised 9 November 2011; accepted 10 November 2011; published 14 January 2012.

[1] Aqueous extracts of secondary organic aerosols (SOA) generated from the ozonolysis of d-limonene were subjected to dissolution, evaporation, and re-dissolution in the presence and absence of ammonium sulfate (AS). Evaporation with AS at pH 4–9 produced chromophores that were stable with respect to hydrolysis and had a distinctive absorption band at 500 nm. Evaporation accelerated the rate of chromophore formation by at least three orders of magnitude compared to the reaction in aqueous solution, which produced similar compounds. Absorption spectroscopy and high-resolution nanospray desorption electrospray ionization (nano-DESI) mass spectrometry experiments suggested that the molar fraction of the chromophores was small (<2%), and that they contained nitrogen atoms. Although the colored products represented only a small fraction of SOA, their large extinction coefficients (>10^5 L mol^{-1} cm^{-1} at 500 nm) increased the effective mass absorption coefficient of the residual organics in excess of 10^3 cm^2 g^{-1} - a dramatic effect on the optical properties from minor constituents. Evaporation of SOA extracts in the absence of AS resulted in the production of colored compounds only when the SOA extract was acidified to pH $\sim$ 2 with sulfuric acid. These chromophores were produced by acid-catalyzed aldol condensation, followed by a conversion into organosulfates. The presence of organosulfates was confirmed by high resolution mass spectrometry experiments. Results of this study suggest that evaporation of cloud or fog droplets containing dissolved organics leads to significant modification of the molecular composition and serves as a potentially important source of light-absorbing compounds.

Citation: Nguyen, T. B., P. B. Lee, K. M. Updyke, D. L. Bones, J. Laskin, A. Laskin, and S. A. Nizkorodov (2012), Formation of nitrogen- and sulfur-containing light-absorbing compounds accelerated by evaporation of water from secondary organic aerosols, *J. Geophys. Res.*, *117*, D01207, doi:10.1029/2011JD016944.

1. Introduction

[2] Monoterpenes ($C_{10}H_{16}$) comprise a significant fraction of biogenic emissions [*Geron et al.*, 2000]. Numerous laboratory, field, and modeling studies have demonstrated that atmospheric oxidation of monoterpenes by O_3 and OH is a globally important source of secondary organic aerosols (SOA) [*Hallquist et al.*, 2009; *Kanakidou et al.*, 2005]. Laboratory measurements have shown that monoterpene SOA efficiently activate cloud and fog droplets due to the high water solubility of the SOA material [*Engelhart et al.*, 2008; *Hartz et al.*, 2005; *van Reken et al.*, 2005]. Likewise, atmospheric modeling studies show that the composition of the aerosol can significantly affect cloud droplet properties [*Ervens et al.*, 2005; *Roesler and Penner*, 2010].

[3] The nuclei of clouds and fogs commonly represent mixtures of organic material and inorganic compounds such as ammonium sulfate, $(NH_4)_2SO_4$ (AS). Once formed, the droplets continue to build up dissolved organic and inorganic material [*Seinfeld and Pandis*, 1998] by wet deposition of water-soluble compounds, including polar organics [*Facchini et al.*, 1999; *Limbeck and Paxbaum*, 2000]; aqueous oxidation of SO_2 to H_2SO_4 [*Finlayson-Pitts and Pitts*, 2000]; cloud-processing of volatile organics [*Carlton et al.*, 2008; *Ervens et al.*, 2008; *Huang et al.*, 2011]; scavenging additional particles; droplet coalescence; and a number of other processes [*Pruppacher and Klett*, 1997; *Seinfeld and Pandis*, 1998]. The total dissolved organic carbon (DOC) content, inorganic ion content, and acidity are greatly enhanced in smaller atmospheric droplets, which alters the chemistry of the droplet [*Barth*, 2006; *Bator and Collett*, 1997; *Chate and Devara*, 2009]. For example, fog water

[1]Department of Chemistry, University of California, Irvine, California, USA.
[2]Chemical and Materials Sciences Division, Pacific Northwest National Laboratory, Richland, Washington, USA.
[3]Environmental Molecular Sciences Laboratory, Pacific Northwest National Laboratory, Richland, Washington, USA.

0148-0227/12/2011JD016944

can have a wide pH range of 2.1–7.6 [*Collett et al.*, 2002; *Mancinelli et al.*, 2005; *Waldman et al.*, 1982], DOC of up to 0.2 g/L [*Capel et al.*, 1990; *Jacob et al.*, 1984; *Mancinelli et al.*, 2005], and sulfate (SO_4^{2-}) and ammonium (NH_4^+) concentrations in excess of 0.15 g/L [*Fisak et al.*, 2002; *Jacob et al.*, 1984; *Joos and Baltensperger*, 1991]. The changes in DOC concentration with droplet size may be induced by, among other things, evaporation in cloud and fog droplets.

[4] When the relative humidity drops and the droplets evaporate, the residual particles contain a mixture of organic and inorganic compounds from the initial droplet nuclei and from the gases and inorganic compounds the droplets picked up during their lifecycle. The processes involving dissolution of particles followed by evaporation of the resulting droplets (cloud cycling) are quite common in the lower atmosphere [*Hoose et al.*, 2008; *Pruppacher and Jaenicke*, 1995]. Furthermore, any given cloud droplet exists on average only a few minutes [*Pruppacher and Klett*, 1997]. The clouds themselves last longer but most of them also dissipate via evaporation on a time scale of hours. "Attempted rains," where droplets scavenge particles and gases during their descent and evaporate without ever hitting the ground, are also quite common [*Lin and Rossow*, 1996; *Rosenfeld and Mintz*, 1988]. Finally, nighttime fogs tend to scavenge soluble material during the night and evaporate in the morning.

[5] The increased concentration and acidity of DOC resulting from evaporation may promote various chemical reactions such as acid-catalyzed processes and condensation reactions that generate water as a reaction product. Chemical processes occurring during evaporation have received little attention from atmospheric chemists despite the fact that aerosols undergo a number of dissolution/evaporation cycles during their lifetime. Previous work focused on evaporation of single-component solutions of glyoxal and methylglyoxal, which was shown to result in formation of involatile oligomeric residues [*De Haan et al.*, 2009b; *Loeffler et al.*, 2006]. So far, there have been no studies of evaporation of solutions containing SOA material or SOA mixed with typical inorganic constituents of clouds and fogs.

[6] Evaporation processes that can produce light-absorbing compounds from the initially colorless SOA organics are of particular interest. Our recent work [*Bones et al.*, 2010; *Laskin et al.*, 2010] demonstrated that biogenic SOA produced by ozone-initiated oxidation of d-limonene undergoes browning as a result of chemical reactions between the carbonyl species in SOA and ammonia. The chromophores formed in these reactions are conjugated nitrogen-containing organic compounds (NOC). These reactions are similar in mechanism to the well-known Maillard browning reaction [*Rizzi*, 1997] between amino acids and reducing sugars. Formation of light-absorbing NOC species has also been observed in the reaction of 1,2-dicarbonyls (glyoxal, methylglyoxal) with hydrated AS aerosols [*Trainic et al.*, 2011], with aqueous solutions of amino acids [*De Haan et al.*, 2009a] and with aqueous solutions of AS [*Galloway et al.*, 2009; *Sareen et al.*, 2010; *Shapiro et al.*, 2009; *Yu et al.*, 2011]. Reactions of photo-oxidized solutions of pyruvic acid mixed with AS also produced colored compounds [*Rincón et al.*, 2009, 2010]. Light-absorbing species can also be produced by mechanisms that do not involve chemistry of reduced nitrogen. For example, photo-oxidation of aromatics under high-NO_x conditions produces aerosol that has intense brown color because of the presence of nitroaromatics [*Jaoui et al.*, 2008]. Aldol condensation of volatile carbonyls under highly acidic conditions results in formation of larger, light-absorbing, unsaturated carbonyls [*Casale et al.*, 2007; *Esteve and Nozière*, 2005; *Garland et al.*, 2006; *Nozière and Esteve*, 2005; *Nozière et al.*, 2006; *Nozière and Esteve*, 2007; *Zhao et al.*, 2005]. Oxidation of hydroxybenzoic acid by Fenton mechanism was shown to produce light-absorbing aromatic compounds [*Gelencsér et al.*, 2003]. As these processes involve condensation reactions, they should be promoted by evaporation, and more generally by low relative humidity conditions. Our previous work demonstrated that condensation oligomers are significantly enhanced in isoprene photooxidation SOA under low relative humidity conditions [*Nguyen et al.*, 2011]. The goal of this work is to examine the possibility of formation of light-absorbing "brown carbon" compounds and other major products during evaporation of aqueous solutions of model biogenic SOA in the presence and absence of AS.

2. Experimental Setup

2.1. Secondary Organic Aerosol Generation

[7] For the majority of experiments, model SOA was produced as previously described [*Bones et al.*, 2010] from the reaction of d-limonene, one of the most common atmospheric monoterpenes [*Geron et al.*, 2000], with ozone in a 17 L glass flow tube at ambient atmospheric pressure (750 $\pm$ 10 Torr), low relative humidity (<2%) and ambient temperature (295 $\pm$ 2 K). Throughout this work, the SOA produced from ozonolysis of d-limonene will be referred to as simply "SOA." d-limonene (Sigma-Aldrich, 97%) was introduced into a flow of zero air and ozone via a syringe pump (Fisher, KDS100) at a rate of 25 μL/hr. The injector was located at the flow cell entrance. Purified air was supplied by a purge gas generator (Parker75- 62), while ozone was produced by flowing oxygen gas (99.994% purity) through a commercial ozone generator. The overall flow through the tube was 3 SLM (standard liters per minute) resulting in a 5–6 min residence time. The estimated steady state limonene mixing ratio in the absence of ozone was 20 ppm, and the measured ozone mixing ratio was around 100 ppm. The 5:1 O_3:limonene ratio was selected to ensure full oxidation of both exo- and endo-cyclic double bonds in limonene [*Maksymiuk et al.*, 2009]. After the flow tube, the resulting mixture was sent through a denuder filled with activated charcoal where excess ozone and volatile organic compounds were removed. The SOA was collected on a pre-weighed filter (Millipore Fluoropore membrane filter, 0.2 μm pore size) at 25 SLM (3 SLM from the cell + 22 SLM of makeup clean air). The filter loading was typically 2–3 mg of SOA material (weighed with Sartorius ME5-F filter balance; $\pm$ 0.001 mg precision) after operating the reactor for approximately 1 h. Additional SOA samples were prepared using lower limonene mixing ratios (300 ppb - 5 ppm), while keeping the O_3:limonene ratio at 5:1, to investigate the effect of the concentrations on the evaporative browning. Finally, some of the samples were also prepared in a 5 m^3 chamber as described by *Bateman et al.* [2011] using limonene mixing ratios below 1 ppm. The chamber-generated SOA had

the same properties as the flow-tube SOA produced at the same limonene and O_3 mixing ratios.

2.2. Dissolution, Evaporation, and Redissolution Experiments

[8] We performed experiments on evaporation of aqueous SOA extracts in the presence and absence of ammonium sulfate (AS) at various pH values. The freshly prepared SOA samples were extracted into ultra-purified water (R ≈18 MΩ-cm, Thermo Barnstead Nanopure) using 15 min sonication to obtain a stock solution with a mass concentration of 0.3 g/L for the dissolved SOA material. We verified the completeness of the filter extraction by performing a secondary extraction of the same filter in water or methanol, which did not dissolve additional organic material, as demonstrated by negligible optical absorption around 200–300 nm (where most organic compounds absorb) of the secondary extract compared to the primary one. A fresh stock solution was prepared for each evaporation experiment and used immediately. A 2 mL aliquot of SOA extract was placed in a 10 mL glass vial. The pH was measured with a digital pH-meter (Mettler Toledo S20) against a calibrated Ag/AgCl reference electrode. The pH of the initial SOA solution at 0.3 g/L was typically 4.5 ± 0.3 reflecting a significant amount of carboxylic acid functionality in SOA. In experiments with AS, a pre-mixed solution of AS was added to the vial to achieve a mass concentration ranging from 0.0003 to 3 g/L (either well below or in excess of the SOA mass concentration of 0.3 g/L). The addition of AS increased the solution pH somewhat (ΔpH < 0.5), depending on the amount added. The pH of the extract was further adjusted to pH = 2–9 by addition of pre-mixed solutions of H_2SO_4 or NaOH. The AS addition, as well as pH adjustments, typically increased the volume of the SOA extracts in the vial by 5–200 μL.

[9] The content of the vial was transferred to a standard 1 cm quartz cuvette, and a UV/Vis absorption spectrum was recorded in a dual-beam spectrophotometer (Shimadzu UV-2450) using ultra-purified water as the reference. The solution was then evaporated to dryness using a rotary evaporator (Buchi R-210) at a bath temperature of T = 50 °C. Because 50 °C is higher than the temperature at which atmospheric cloud and fog droplets normally evaporate, we first investigated the effect of the temperature on the extent of browning. Figure S1 in the auxiliary material shows that the chromophore concentration increased by about 30% when the temperature was reduced from 50 °C to 25 °C in our evaporation experiments.[1] Despite this temperature effect, T = 50 °C bath temperature was chosen to reduce the evaporation time of relatively large sample volumes (2–3 mL). For example, it takes <10 min to evaporate 2 mL from the vial at T = 50 °C as opposed to >60 min at 25 °C. As water was always present in the parts of the evaporator that were at room temperature and the pumping rate was relatively low, the pressure in the evaporator was around 15–20 Torr during the evaporation experiments, and it was dominated by the water vapor. This corresponds to about 16–22% relative humidity in the vial at the end of the evaporation (equilibrium water vapor pressure at 50 °C is 93 Torr). We will come back to this point when we discuss the atmospheric implications of this work.

[10] After evaporation, the residue was redissolved in ultra-purified water to achieve the original SOA concentration of 0.3 g/L, and the UV/Vis absorption spectrum of the resulting solution was recorded, thus completing the dissolution/evaporation/redissolution cycle. The redissolution step was necessary in our experiments in order to quantitatively compare optical properties of the water-soluble organics before and after evaporation, and investigate the stability of the chromophores with respect to hydrolysis. For each set of pH and AS concentrations, the experiment was repeated 2–4 times using different SOA batches in order to assess the degree of variability in the results. Uncertainties are reported within one standard deviation.

[11] We quantify the degree of browning in terms of the effective average mass absorption coefficient (*MAC*, measured in the units of $cm^2\ g^{-1}$) of the organic material, which can be directly calculated [*Chen and Bond*, 2010] from the base-10 absorbance A_{10} of an SOA extract with the solution mass concentration C_{mass} (g cm^{-3}) measured over path length b (cm):

$$MAC(\lambda) = \frac{A_{10}^{solution}(\lambda) \times \ln(10)}{b \times C_{mass}} \quad (1)$$

It is also convenient to define $\langle MAC \rangle$ averaged over the desired wavelength range, typically from 300 to 700 nm:

$$\langle MAC \rangle_{\lambda_1-\lambda_2} = \frac{1}{\lambda_2 - \lambda_1} \times \int_{\lambda_1}^{\lambda_2} MAC(\lambda) d\lambda \quad (2)$$

For the sake of consistency, we only included the mass concentration of the organic material in equations (1) and (2), and excluded the mass concentration of the inorganic additives (AS, H_2SO_4, and NaOH).

[12] We found that the calculated $\langle MAC \rangle$ depended weakly on the initial limonene mixing ratio used in SOA preparation for SOA extracts examined at 0.3 g/L mass concentration. For example, $\langle MAC \rangle$ for evaporated samples with AS ("brown samples") increased by about 30% between the experiments using the lowest (300 ppb) and the highest (20 ppm) limonene mixing ratios. We have not corrected the measured values for these concentration effects. In view of the observed SOA precursor concentration dependence, the *MAC* values reported here should be treated as an upper limit to the *MAC* expected for atmospherically relevant limonene concentrations.

2.3. High Resolution Mass Spectrometry Analysis

[13] The solutions were analyzed before and after evaporation using a high-resolution LTQ-Orbitrap™ mass spectrometer (Thermo Electron Corporation, Inc.) equipped with an electrospray ionization (ESI) source. Acetonitrile (ACN, Aldrich, >99.9%) was added to the solutions to improve the stability of the ESI. The dry residue formed in the evaporation was also analyzed using a home-built nano-DESI source described by *Roach et al.* [2010]. For nano-DESI experiments, a droplet of the solution was placed on the surface of a microscope slide and evaporated to dryness with gentle heating. Blank mass spectra were obtained from the

[1] Auxiliary materials are available in the HTML. doi:10.1029/2011JD016944.

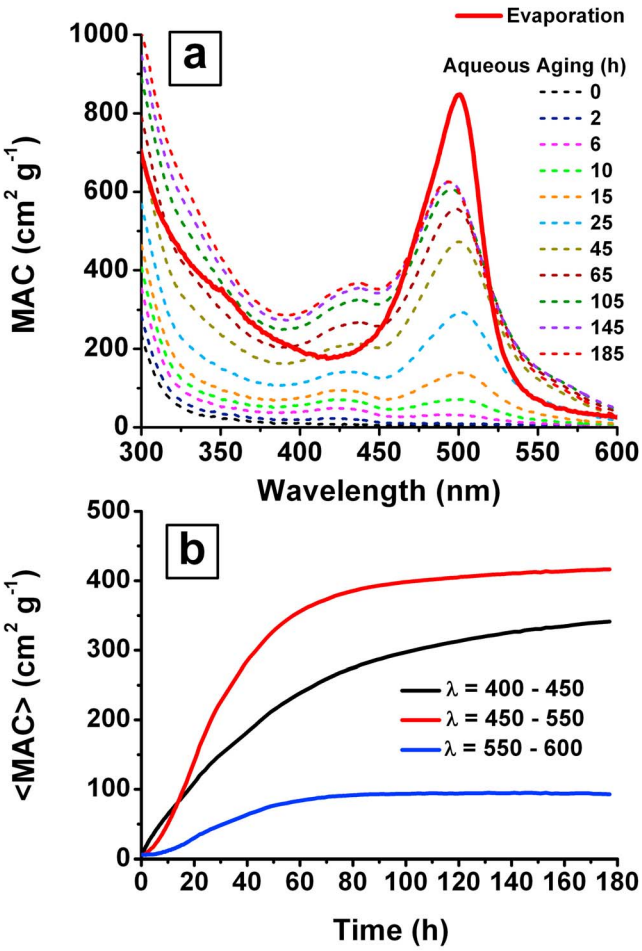

Figure 1. (a) Comparison of the absorption spectra of a solution containing 0.3 g/L of SOA and 0.3 g/L of AS at different reaction times (dashed lines) with the absorption spectrum of the evaporated/redissolved sample obtained after subtraction of the pre-evaporated spectrum (solid red line) with the same initial concentrations. (b) The time dependence of the average *MAC* values corresponding to the 400–450, 450–550, and 550–600 nm windows. The aqueous system does not reach the same absorbance as the evaporated one, and the absorbances keep growing even after 5 days of reaction. The shapes of the absorption spectra are different, reflecting differences in the reaction mechanisms.

unexposed microscope slide surface, which were not significantly different from the mass spectra of the working solvent itself. The H_2O/ACN solvent for the nano-DESI or the probe solution for the ESI were fed through a fused silica capillary tip (50 μm ID) at a flow rate of 0.5–1.0 μL min^{-1}, using a spray voltage of about 4.0 kV. The system was operated in both positive and negative ion modes with a resolving power of 60,000 (m/Δm at *m/z* 400) and a mass range of *m/z* 100–2000. Calibration was done twice a day using a standard solution composed of caffeine, MRFA and Ultramark 1621 (calibration mix MSCAL 5, Sigma–Aldrich, Inc).

[14] Data analysis was similar to that described in our previous publications on high resolution mass spectra of limonene SOA [*Bateman et al.*, 2009; 2011; *Laskin et al.*, 2010; *Walser et al.*, 2008]. After the calibration, the mass accuracy was better than $\pm$0.001 Da across the *m/z* rage of 100–1000. Peaks that appeared only in the mass spectra of the solvent or blank samples were discarded. Peaks in the positive ion mode spectra (for the samples evaporated with AS) were assigned to formulas $C_cH_hO_oN_{0-2}S_{0-2}Na^+_{0-1}$ while peaks in the negative ion mode spectra (for the samples evaporated with H_2SO_4) were assigned to $C_cH_hO_oN_{0-2}S^-_{0-2}$. The formula assignment procedure did not allow ions to have both N and Na atoms (under the assumption that molecules contacting reduced nitrogen should have high proton affinities). The H/C and O/C ratios were limited to 0.8–2.1 and 0.1–1.5, respectively. Ambiguous assignments were evaluated by checking mass defects, parities, atomic ratios, and double bond equivalents (DBE) [*Nizkorodov et al.*, 2011].

3. Results and Discussion

3.1. Evaporation of Limonene SOA in the Presence of AS

[15] Evaporation of limonene SOA solutions in the presence of AS reproducibly generated a brown residue in the evaporation vial. The solution remained colorless during the initial stages of evaporation, with the color change occurring over a short period of time, usually in less than a minute, as the residual water was removed from the sample. The residue was fully soluble in water and the resulting solution maintained its brown color for many hours, indicating that the chromophores were stable with respect to hydrolysis (auxiliary material Figure S2).

[16] The solid red trace in Figure 1a shows a typical UV/Vis absorption spectrum obtained by subtracting the pre-evaporation spectrum of an SOA + AS extract (pH = 4.5) from the post-evaporation/redissolution spectrum. Because the initial SOA + AS solutions do not absorb significantly above 300 nm, the difference spectra in the 300–700 nm range are entirely due to the chromophores generated during the evaporation. All of the absorption spectra presented in Figure 1 and thereon correspond to the difference spectra converted into *MAC* units using equation (1).

[17] The evaporated/redissolved SOA+AS extracts have a distinctive absorption band at around 500 nm superimposed on a broad absorption that smoothly increases toward UV. Similar absorption spectra were obtained at other pH values, as discussed below. A similar 500 nm absorption band appeared in the slow SOA + AS chemistry occurring in the bulk aqueous phase on a timescale of hours to days [*Bones et al.*, 2010]. This band was also observed when limonene SOA collected on a substrate was exposed to humid air containing ammonia (NH_3) [*Laskin et al.*, 2010]. Comparison of the absorption spectra suggests that the general features of the browning mechanism are similar for the SOA +AS (solution), SOA + AS (evaporated solution), and SOA + NH_3 (gas -particle) cases. *Bones et al.* [2010] also studied the reaction between amino acids and SOA in the aqueous phase. From the amino acid dependent shifts in the position of the 500 nm absorption band, it was concluded that the chromophores were likely nitrogen-containing organic compounds (NOC). Evaporation experiments in which AS was replaced by glycine also resulted in a significant red shift in the position of the 500 nm band (auxiliary material

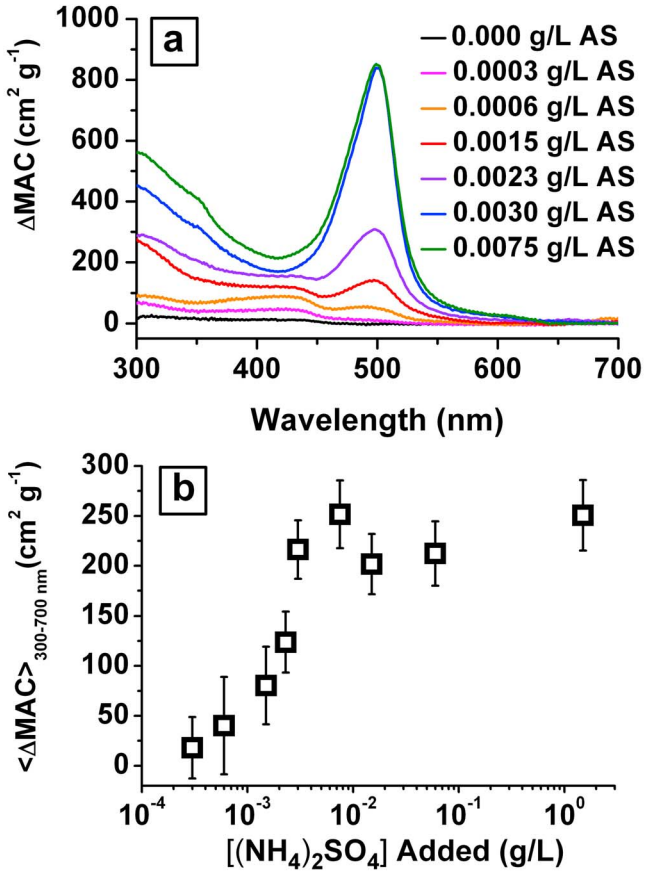

Figure 2. The effect of the initial AS mass concentration on (a) the absorption spectra and (b) the $\langle \Delta MAC \rangle_{300–700nm}$ values of the evaporated/redissolved SOA + AS solutions. The SOA mass concentration is 0.3 g/L in all cases. The absorbance saturates above the relative AS:SOA mass ratio of 1:100. The C_{430} chromophore is favored at low AS concentrations, but the C_{500} chromophore becomes dominant above this saturation ratio.

Figure S3), confirming that the 500 nm chromophores formed during the evaporation also correspond to NOC.

[18] However, there are also reproducible differences in the chemistry between the aqueous and evaporation aging experiments. The dashed traces in Figure 1a correspond to the UV/Vis absorption spectra for the aqueous mixture containing 0.3 g/L SOA and 0.3 g/L AS, obtained as a function of reaction time in bulk solution. When compared with the spectrum obtained by evaporation and redissolution of the same mixture (solid red line), it is obvious that the evaporation chemistry produces chromophores absorbing in the 500 nm region on an accelerated timescale. In aqueous solutions of limonene SOA aged with AS, the 500 nm absorption band and another absorption band at 430 nm slowly form over the course of ~180 h. There is an additional shoulder at 570 nm, which becomes discernable after 2 days of reaction. For brevity, chromophores absorbing at λ = X nm will be referred to henceforth as C_X.

[19] The spectral position of C_{430} continuously shifts toward the red (from $\lambda_{max} \sim 425$ nm at early times to ~440 nm after 180 h) and the position of C_{500} continually shifts toward the blue (from $\lambda_{max} \sim 505$ nm at early times to ~490 nm after 180 h) throughout the experiment, possibly due to additional peaks growing in the same spectral region or/and slow aqueous oxidation of the chromophores. Such slow reactions should not, and does not, affect the chromophores in the evaporated/redissolved samples, which are produced and analyzed on a considerably shorter experimental timescale (minutes). In contrast, C_{430} is not visible in the spectrum of the evaporated sample (this band does appear in the evaporated solutions at considerably lower AS concentrations, see below). The shape of C_{500} is considerably narrower in the evaporated sample, and there is no evidence of the C_{570} shoulder band. It appears that the slower SOA + AS aqueous chemistry produces a considerably wider range of chromophoric compounds, and evaporation selectively favors the compounds absorbing at 500 nm.

[20] *Bones et al.* [2010] compared the UV/Vis spectra of AS + excess SOA and SOA + excess AS in bulk solution after 20 h of reaction. The absorption of C_{430} was significantly stronger in the AS + excess SOA case, which led to the suggestion that C_{430} are either imine-based intermediates in the formation of C_{500} or formed in an NH_4^+-catalyzed reaction. In this work, the kinetics of C_{430} and C_{500} were followed over a significantly longer time scale (Figure 1b), and the results are more consistent with NH_4^+ catalysis to form C_{430} and N-incorporation to form C_{500}. In order to account for the slow shift in the peak positions, the time dependence data presented in Figure 1b were averaged over the 400–450 nm range for C_{430}, the 450–550 nm range for C_{500}, and the 550–600 nm for C_{570}. The growth of C_{500} and C_{570} follows sigmoidal time dependence, which is consistent with the sequential "SOA compound → intermediate → chromophore" mechanism. The kinetics of C_{500} could be fitted with the effective first order rate constants of 0.044 and 0.090 h^{-1} for the two sequential steps. The observed growth of C_{430} could be well described with a single effective rate constant of 0.019 h^{-1}. Because of its slower rate of formation, C_{430} continues to grow after 180 h when C_{500} and C_{570} are close to saturation. The difference in the rate constants indicates that C_{430} is not an intermediate in the formation of C_{500} or C_{570}; they are formed by independent mechanisms.

[21] The dependence of the chromophore production on the AS concentration in the evaporation/redissolution experiments was examined by varying the initial mass concentration of AS (= $[AS]_{mass}$) relative to that of SOA by several orders of magnitude from $[AS]_{mass}$:$[SOA]_{mass}$ = 1:1000 to 10:1. The $[SOA]_{mass}$ remained fixed at 0.3 g/L in these experiments. Although the addition of AS increased the solution pH to 4.5 – 5.0, we have not compensated for this because the browning chemistry does not change significantly over this pH range (see below).

[22] Figure 2a shows the dependence of the absorption spectrum of the evaporated/redissolved SOA + AS solution on the initial $[AS]_{mass}$ (Figure S4 shows a photograph of the corresponding solutions, with different shades of brown). There is a distinction between absorption spectra in the low $[AS]_{mass}$ and higher $[AS]_{mass}$ range: small concentrations of AS lead to an exclusive formation of C_{430}, whereas higher concentrations of AS suppress C_{430} in favor of C_{500}. Figure 2b shows the $\langle MAC \rangle_{300–700nm}$ of the evaporated/redissolved sample as a function of the initial $[AS]_{mass}$.

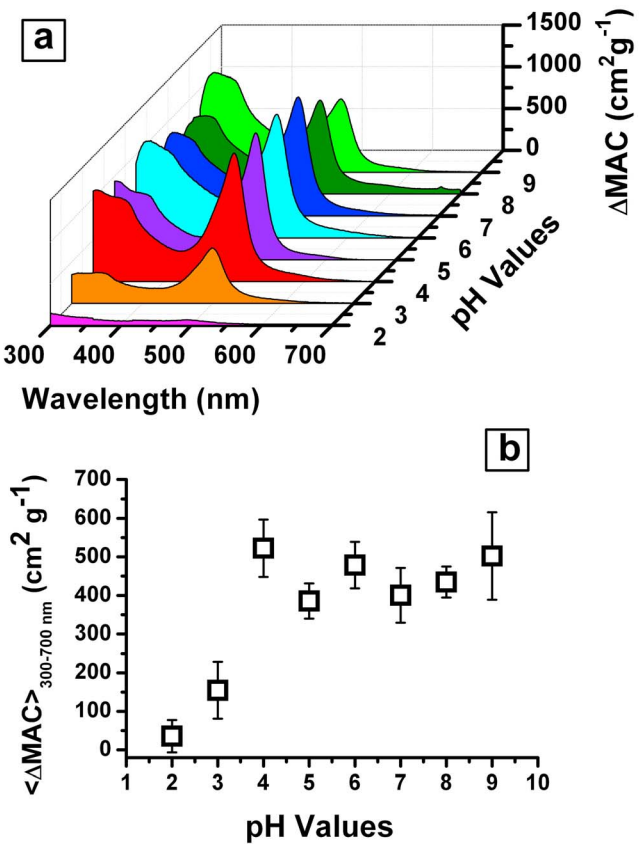

Figure 3. (a) Absorption spectra observed after evaporation/redissolution of SOA + AS solutions at different initial pH. The absorbance was converted into *MAC* units using equation (1). (b) $\langle \Delta MAC \rangle_{300-700nm}$ were calculated from equation (2). The reaction between SOA and AS appears to be suppressed under acidic conditions.

At the lower $[AS]_{mass}$, both C_{430} and C_{500} contribute to $\langle MAC \rangle_{300-700nm}$, with C_{500} absorption becoming dominant at higher $[AS]_{mass}$, in good agreement with the observations of *Bones et al.* [2010] in the aqueous phase.

[23] Remarkably, the $\langle MAC \rangle_{300-700nm}$ values reach a plateau after the $[AS]_{mass}$:$[SOA]_{mass}$ ratio exceeds 1:100. Assuming an average molecular weight of 300 g/mol for limonene SOA compounds, this translates into an effective molar ratio of AS:SOA of 0.022. Further assuming that each AS molecule may supply two NH_4^+ ions for reaction with SOA compounds to produce C_{500}, we estimate that <2% of SOA compounds are converted into C_{500}. It is of course entirely possible that additional SOA compounds undergo competing reactions with NH_4^+, which do not lead to products absorbing in the visible region, or that C_{500} contains more than one nitrogen atom. Such reactions would lower the estimate of the molar fraction of SOA compounds capable of generating brown products even further. Using the same assumptions, we can also place the lower limit for the molar extinction coefficient of the chromophores as $>10^5$ L mol^{-1} cm^{-1} at 500 nm. We conclude that the *MAC* of the browned SOA mixture is dominated by a very small number (<2%) of very strong absorbers, with the rest of the SOA compounds absorbing little or no visible light. We will come back to this important point during the discussion of the atmospheric relevance of these results.

[24] The dependence of C_{430} and C_{500} formation on $[AS]_{mass}$ further supports the hypothesis that they are produced by different mechanisms. Our observations are qualitatively consistent with an AS-catalyzed formation of C_{430}, and with a two-stage mechanism of C_{500} production, which must involve a reaction with AS in one of these steps to produce an NOC with at least one nitrogen atom:

$$\text{(R1)} \qquad SOA_1 \ (+AS)_{catalyzed} \rightarrow C_{430}$$

$$\text{(R2a)} \qquad SOA_2 \ (+AS)_{catalyzed} \rightarrow \text{Intermediate}$$

$$\text{(R2b)} \qquad \text{Intermediate} + AS \rightarrow C_{500}$$

Catalysis by NH_4^+ has been documented in certain reactions involving carbonyls such as aldol condensation [*Dziedzic et al.*, 2009; *Nozière et al.*, 2010a] leading to the formation of oligomeric and fulvic-like compounds [*Nozière et al.*, 2009]. Based on experiments conducted in this study, it is likely C_{430} is nitrogen-free (although we do not have enough evidence to completely rule out direct reaction with NH_4^+). At higher AS concentrations, production of the NOC chromophore C_{500} becomes more favorable because the exponential dependence of C_{500} formation on [AS] is amplified at higher $[AS]_{mass,}$ resulting in the almost exclusive formation of the 500 nm chromophore.

[25] Regardless of the formation mechanism for the light-absorbing products, it is clear that evaporation significantly accelerates the formation of chromophores, mainly C_{500}, with respect to the aqueous phase. It takes >150 h for the bulk aqueous chemistry to reach *MAC* values in the 500 nm region comparable to what can be achieved in a 10 min evaporation/redissolution experiment. The reaction is effectively accelerated by approximately 3 orders of magnitude. Because the color change takes place in less than one minute during the last stages of the evaporation, the actual rate enhancement is even greater. Considering the widespread nature of droplet evaporation events in the atmospheric environment, this kind of evaporation-driven chemistry has a real potential to irreversibly modify light absorbing properties and chemical composition of the dissolved organic material.

[26] The evaporation/redissolution experiments were performed at different initial pH values to confirm that the evaporation-induced browning occurs under atmospherically relevant conditions. Figure 3a shows absorption spectra and Figure 3b shows $\langle MAC \rangle_{300-700nm}$ values for the evaporated/redissolved SOA + AS sample as a function of the initial solution pH. The average *MAC* values are of the order 500 cm^2 g^{-1}, and the peak values (at 500 nm) are in excess of 10^3 cm^2 g^{-1}. At pH values below 4, the browning is inhibited. The suppression of the NH_4^+ -induced chromophore formation under acidic conditions was also observed in the bulk solutions of carbonyls + AS [*Nozière et al.*, 2009; *Shapiro et al.*, 2009] and limonene SOA + AS reaction [*Bones et al.*, 2010]. It is notable that in the absence of AS, SOA extracts acidified by H_2SO_4 at pH = 2 do produce light-

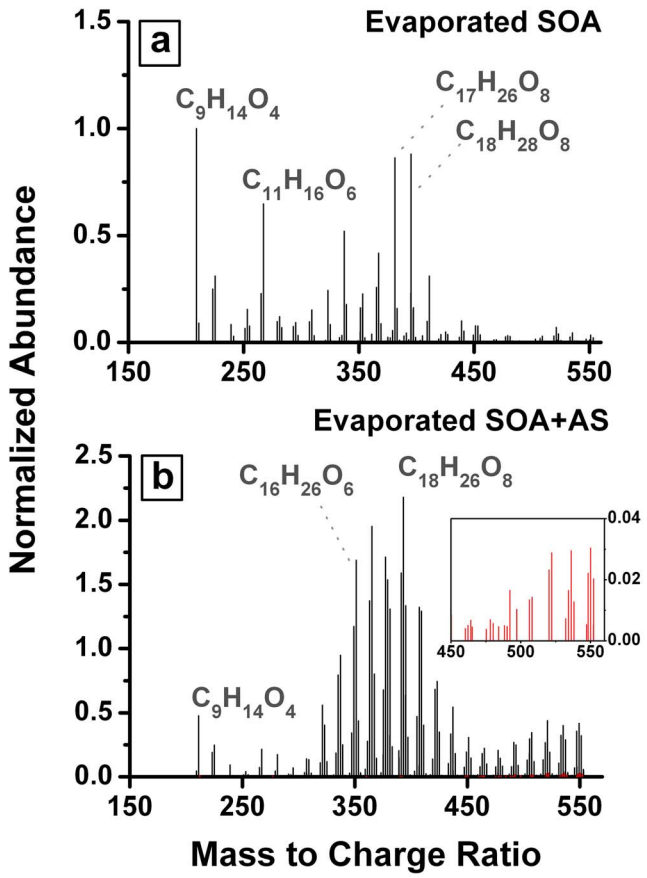

Figure 4. Positive ion mode nano-DESI mass spectra of evaporated SOA residues obtained (a) without AS and (b) with AS. Red peaks correspond to formulas containing nitrogen (magnified in the insert). Selected peaks are labeled with the formulas of the corresponding neutral molecules. Peak intensities of both spectra were normalized to the intensity of the sodiated $C_9H_{14}O_4$ (*m/z 209*.0784) found in the evaporated SOA spectrum.

absorbing compounds upon evaporation (see section 3.3). However, the AS+H_2SO_4+SOA solutions at pH = 2 do not show significant browning during evaporation. Mixtures of H_2SO_4 and AS have complex phase diagrams [*Chelf and Martin*, 1999; *Martin*, 2000] and may form solid phases corresponding to $(NH_4)_zH_{[2-z]}SO_4$ (z = 2 for ammonium sulfate, 1 for ammonium bisulfate, 1.5 for letovicite) upon removal of water. Formation of these solid phases in the evaporated AS + H_2SO_4 + SOA system may bind the H^+ and NH_4^+ ions and make them unavailable for participation in the browning reactions that occur in the evaporated H_2SO_4+SOA system at pH = 2 and in the AS + SOA system at pH ≥ 4. The shape of the absorption spectrum does not significantly change in the range of pH = 4–9 (Figure 3a), suggesting that the addition of NaOH to increase the pH does not significantly alter the chemistry.

3.2. Composition of Evaporated SOA Extracts in the Presence of AS Studied With High-Resolution Mass Spectrometry

[27] Evaporation of solutions of methylglyoxal in the presence of amino acids was found to form oligomers of NOC, which were strongly light-absorbing [*De Haan et al.*, 2009a]. Aqueous solutions of AS mixed with glyoxal or methylglyoxal [*Galloway et al.*, 2009; *Sareen et al.*, 2010; *Shapiro et al.*, 2009; *Yu et al.*, 2011], and AS mixed with pyruvic acid [*Rincón et al.*, 2009, 2010] were also shown to undergo browning and form complex NOC simultaneously. Our previous experiments on aqueous reactions of limonene SOA with amino acids and AS demonstrated that C_{500} is a light-absorbing NOC based on evaporated (auxiliary material Figure S3) and aqueous [*Bones et al.*, 2010] experiments. Because chromophores produced during evaporation of limonene SOA + AS solutions and in the bulk aqueous phase have similar absorption spectra, we expected to observe a significant fraction of NOC in the mass spectra of the dry residues.

[28] Figure 4 shows the nano-DESI mass spectra of the evaporated SOA residues produced in the absence (Figure 4a) and presence (Figure 4b) of AS. The spectra include only compounds for which the elemental composition could be unambiguously assigned. Selected high-abundance peaks are labeled with the formula of the corresponding SOA compound. Peak intensities were normalized with respect to a known major limonene/O_3 oxidation product, sodiated keto-limononic acid [*Bateman et al.*, 2009; *Walser et al.*, 2008] ($C_9H_{14}O_4Na^+$, *m/z 209.079*). The same normalization was applied to the evaporated AS + SOA spectrum (although the intensities are not easily comparable between nano-DESI spectra of different samples). The spectra are not dramatically different between the samples evaporated with and without AS. However, the fraction of higher-MW compounds is larger in the former. Although the contribution of NOC compounds increased from 2% to 11% by count (auxiliary material Table S1) when evaporation was done with AS, the contribution of NOC to the total ion current (TIC) was <1%. A negligible fraction (<1% by count) of compounds in the evaporated AS + SOA sample could be assigned to sulfur-containing organic compounds (SOC). No SOC appeared in the evaporated SOA sample without AS, as expected.

[29] The fraction of NOC in the evaporated SOA+AS residues appears to be surprisingly small. *Bones et al.* [2010] also found little change in the ESI mass spectra and no evidence of extensive production of NOC in the SOA + AS solutions after they browned. These observations are consistent with the "titration" experiment shown in Figure 2, which suggested that less than ∼2% of the SOA compounds participate in the production of chromophores in reactions with AS. It is remarkable that the optical characteristics of SOA material can change so drastically without an accompanying change in the overall molecular composition.

[30] The low NOC fraction observed in the AS + SOA case should be contrasted to the previous DESI and ESI MS study, which detected a significantly higher fraction of NOC in the mass spectra of limonene SOA immobilized on a substrate and exposed to humid NH_3 vapor [*Laskin et al.*, 2010]. It appears that gaseous ammonia is more efficient at producing NOC than AS. Indirect support for this hypothesis comes from our measurements of *MAC* for different types of organic aerosols aged with humid NH_3 vapor. That study showed that $\langle MAC \rangle_{300-700nm}$ values of limonene SOA exposed to humid NH_3 vapor exceed *MAC* for the dissolved/evaporated SOA+AS sample by a factor of ∼2, with an array

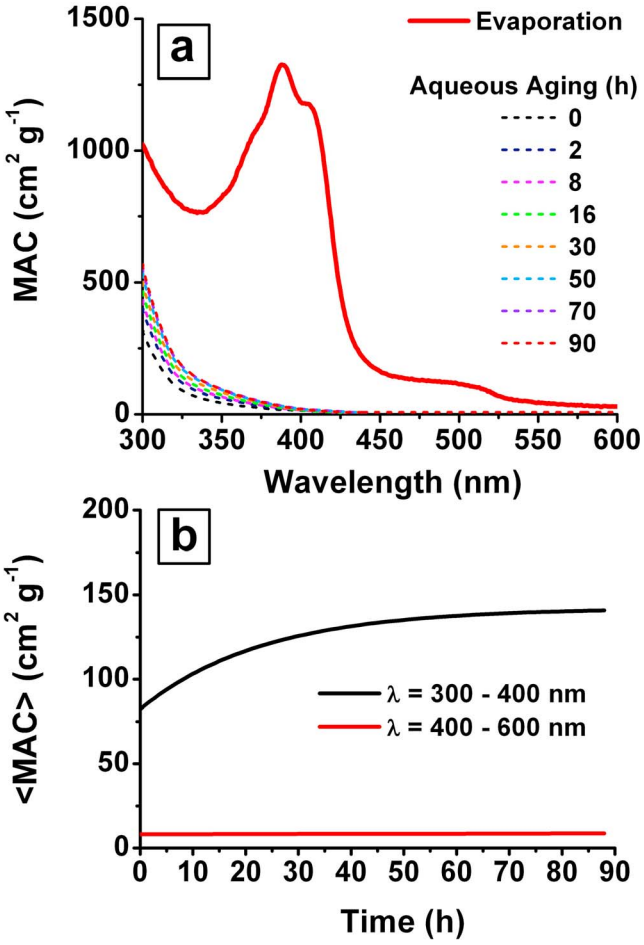

Figure 5. (a) Comparison of the evolution of absorption spectra over time of a solution containing 0.3 g/L of SOA, acidified to pH = 2 with H_2SO_4, with the absorption spectrum of the evaporated/redissolved sample with the same initial concentrations. The evaporation chemistry is distinctly different from the aqueous chemistry, where no visible light-absorbing compounds are produced. (b) The time dependence of the average *MAC* values corresponding to the 300–400 nm and 400–600 nm windows.

of NOC compounds detectable by nano-DESI. In order to keep this paper focused on evaporation, the results of the SOA + humid NH_3 vapor study will be presented elsewhere.

3.3. Evaporation of Limonene SOA Acidified by H_2SO_4

[31] Evaporation and redissolution experiments for SOA + H_2SO_4 (or NaOH) mixtures were performed over a range of initial pH values. The evaporation of SOA solutions in the pH range of 3–9 did not produce light-absorbing species. However, SOA solutions acidified with H_2SO_4 to pH = 2 produced oily red-brown residues after evaporation. Unlike the SOA + AS case, the residue was only partially soluble in water (auxiliary material Figure S5 shows that water extracted a smaller fraction of light-absorbing organics from the residue compared to acetonitrile and tetrahydrofuran). Similar to the SOA + AS case, the water-soluble chromophores formed in the SOA+H_2SO_4 reaction were stable with respect to hydrolysis on a time scale of at least a day (see auxiliary material Figure S6). In this study we examined the water soluble fraction by UV/Vis spectroscopy, and the water/acetonitrile soluble fraction with high resolution ESI mass spectrometry.

[32] In the absence of AS, evaporation of acidic aqueous solutions promotes the production of light-absorbing compounds that would not be produced otherwise in the aqueous phase chemistry. Figure 5 compares the evolution of the absorption spectrum during slow aqueous-phase chemistry of pH = 2 SOA extracts with the spectrum obtained after evaporation/redissolution. In the SOA + AS system, the aqueous-phase chemistry slowly produced absorption spectra that were qualitatively similar to the spectra resulting from evaporation (Figure 1). In contrast, the aqueous-phase reactions in SOA + H_2SO_4 (pH = 2) system do not produce light-absorbing compounds without evaporation, except for small changes occurring in the near-UV region.

[33] Figure 6a shows absorption spectra of the evaporated SOA as a function of pH (H_2SO_4 and NaOH were used for pH adjustment). Chromophoric compounds are produced at pH = 2, as evidenced by overlapping absorption peaks at

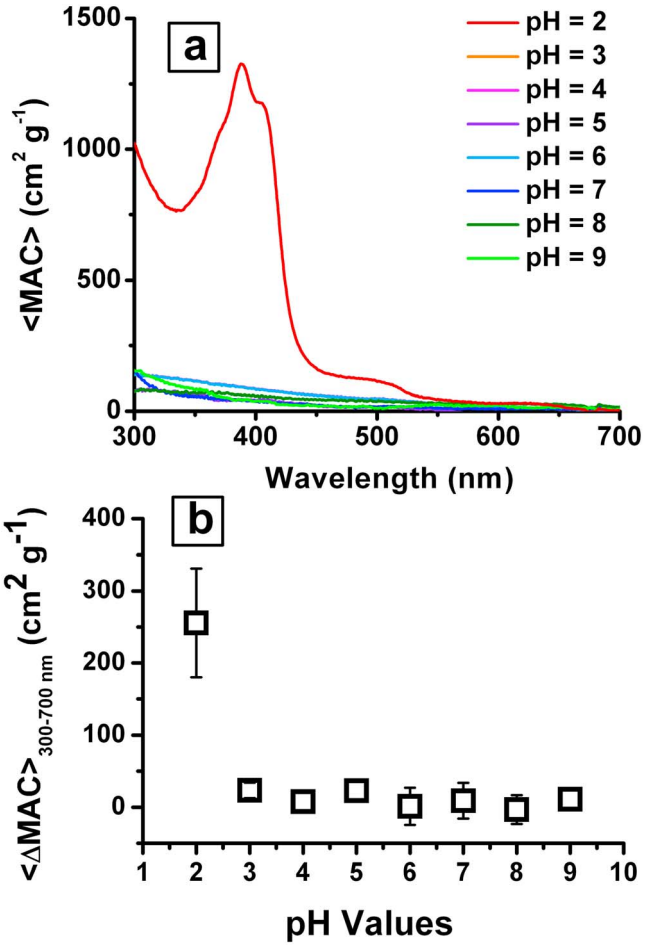

Figure 6. (a) Absorption spectra observed after evaporation/redissolution of SOA + H_2SO_4 solutions at different initial pH values. The absorbance was converted into *MAC* units using equation (1). (b) $\langle \Delta MAC \rangle_{300-700nm}$ was calculated from equation (2). Unlike the AS+SOA evaporation case, browning is more efficient under acidic conditions.

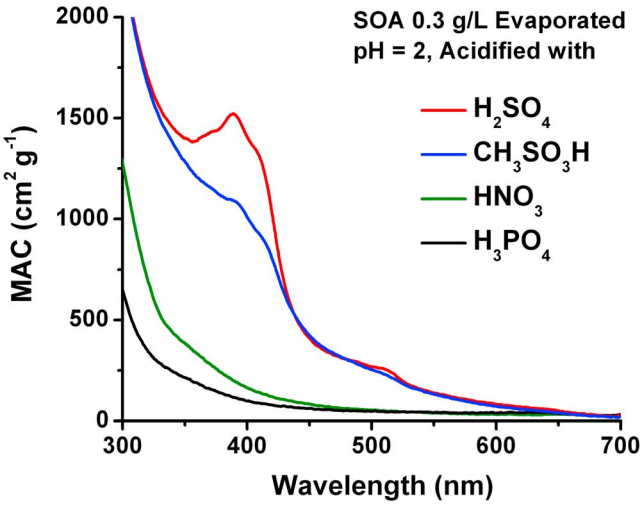

Figure 7. Absorption spectra (converted into *MAC*) observed after evaporation of SOA solutions acidified to pH = 2 with various acids, followed by redissolution in water. The change in the positions of the absorption bands for the sulfuric and methanesulfonic acids provides indirect evidence for the incorporation of S atoms in the chromophores.

390 nm and 410 nm. There is also a small peak at 510 nm that becomes more readily observable in spectra taken in acetonitrile (auxiliary material Figure S7). Figure 6b demonstrates that the $\langle MAC \rangle_{300-700nm}$ values decrease sharply at pH > 2 from approximately 250 $cm^2\ g^{-1}$ to <50 $cm^2\ g^{-1}$. Based on the comparison of the UV/Vis spectra in Figures 3 and 6, and on the observed pH dependence, it is clear that the chemistry governing the production of chromophores in the experiments with H_2SO_4 is starkly different from that occurring in the experiments with AS. For example, both the 430 nm and 500 nm bands found in SOA + AS evaporated residues are absent in the SOA +H_2SO_4 spectra in Figure 6a. Lower pH suppresses browning in the SOA + AS case and enhances it in the SOA +H_2SO_4 case.

[34] The mechanism of chromophore production from the evaporation of SOA extracts with H_2SO_4 may be similar to the acid-catalyzed aldol condensation reaction of carbonyl compounds in solutions of concentrated H_2SO_4 [*Garland et al.*, 2006; *Nozière and Esteve*, 2005; *Nozière et al.*, 2007; *Nozière and Esteve*, 2007]. The active removal of water during the evaporation and simultaneous increase in the acidity both help shift the equilibrium from reactants toward the aldol condensation products. A large fraction of the compounds in limonene ozonolysis SOA are carbonyls. For example, *Bateman et al.* [2008] previously estimated that at least 40% of the SOA compounds are either ketones or aldehydes. The high concentration of acid coupled to the removal of water may catalyze the production of light-absorbing aldol products in the evaporated samples, similar to the results obtained in the reactions of simple C_2-C_8 carbonyls with concentrated H_2SO_4 solutions [*Casale et al.*, 2007; *Garland et al.*, 2006; *Nozière and Esteve*, 2005; *Nozière et al.*, 2007; *Nozière and Esteve*, 2007]. Although the 390 nm and 410 nm absorption bands observed in this work do not exactly match the bands produced in H_2SO_4-catalyzed reactions of C_2-C_8 carbonyls, the wavelength range over which absorption happens (350–450 nm) is the same. The carbonyls found in limonene SOA are larger (>C_8) and multifunctional. The average molecular "formula" for the monomeric limonene/O_3 SOA compounds can be best expressed as $C_{10}H_{16}O_4$, containing 2–4 oxygenated functional groups per molecule [*Bateman et al.*, 2009; *Walser et al.*, 2008]. Therefore, the aldol condensation products in the limonene SOA are expected to be highly substituted, with a higher degree of conjugation and different absorption properties as compared to the aldol condensates formed from the simpler carbonyls.

[35] Acidity alone does not fully explain the formation of light-absorbing compounds. We conducted experiments in which H_2SO_4 was replaced by either nitric acid (HNO_3), phosphoric acid (H_3PO_4), or methanesulfonic acid (CH_3SO_3H, MSA). Evaporation of SOA solutions acidified at pH = 2 with HNO_3 and H_3PO_4 did not result in visible browning or the production of C_{390}, C_{410} or C_{500} bands observed in evaporation/redissolution of the SOA + H_2SO_4 mixtures (Figure 7). More significantly, replacing H_2SO_4 by MSA produced a small wavelength shift in the positions of the C_{390} and C_{410} bands, in both the water soluble fraction (Figure 7) and in the fraction that dissolved in acetonitrile (auxiliary material Figure S7), implying that these chromophores are sulfur-containing organic compounds (SOC). We will show in the next section that evaporation of the SOA+H_2SO_4 solutions is accompanied by formation of a number of organosulfates. While the $-OS(O)_2OH$ and $-OS(O)_2CH_3$ groups are not chromophoric by themselves, incorporation of these groups next to the chromophoric core of a molecule may change its optical properties. Based on these observations, we conclude that the chromophores formed during evaporation of the SOA + H_2SO_4 solutions are SOC, and the presence of sulfur affects their optical properties.

3.4. Composition of Evaporated SOA Extracts Acidified by H_2SO_4 Studied With High-Resolution Mass Spectrometry

[36] The same conditions that favor production of aldol condensates in evaporating SOA + H_2SO_4 solutions are also favorable for production of organosulfates (H_2SO_4 esters). Organosulfates represent an important fraction of atmospheric aerosols. They have been observed in field studies of aerosols [*Chan et al.*, 2010; *Gómez-González et al.*, 2008; *Hawkins et al.*, 2010; *Reemtsma et al.*, 2006; *Schmitt-Kopplin et al.*, 2010; *Surratt et al.*, 2007] and in laboratory SOA generated in the presence of acidic seeds [*Iinuma et al.*, 2007a, 2007b, 2009; *Liggio and Li*, 2006]. They can also be generated by aqueous photolysis of organics in the presence of sulfates [*Nozière et al.*, 2010b]. In particular, oxidation of limonene by ozone has been demonstrated to produce organosulfate oligomers on acidified seeds [*Iinuma et al.*, 2007b]. However, no accompanying color change was reported in these experiments.

[37] Direct esterification of alcohols is one possible route to organosulfates

$$\text{(R3)} \qquad R{-}OH + H_2SO_4 \rightarrow R{-}OS(O)_2OH + H_2O$$

but it is believed to be too slow under most atmospherically relevant conditions [*Darer et al.*, 2011; *Minerath et al.*,

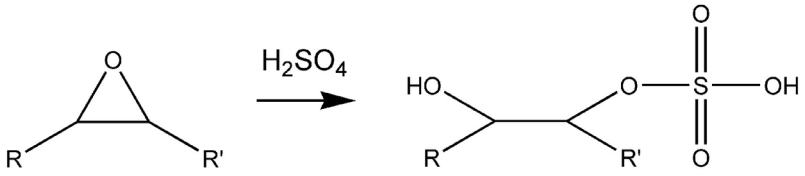

Figure 8. Reaction (4).

2008; *Minerath and Elrod*, 2009]. It should be noted that enolic forms of carbonyls may contribute to R-OH in reaction (R3) and in the case of deliquesced particles, the keto-enol tautomerism equilibrium may be shifted toward the enol, enhancing direct esterification [*Ghorai et al.*, 2011]. Additionally, organosulfates may be formed in the more kinetically favorable ring-opening reaction of epoxides by H_2SO_4, as proposed in a number of previous studies, e.g., see [*Darer et al.*, 2011; *Eddingsaas et al.*, 2010; *Minerath and Elrod*, 2009] and references therein. Both reactions (R3) and (R4) (Figure 8) are acid-catalyzed and therefore should be accelerated by evaporation in the presence of acids. Reaction (R3) is a condensation process and should additionally benefit from the active removal of water during evaporation.

[38] We examined the composition of the redissolved evaporation residues with high-resolution mass spectrometry using negative ion mode ESI. Figure 9 shows assigned peaks in the mass spectra of evaporated/redissolved limonene SOA (Figure 9a), limonene SOA + H_2SO_4 at pH = 4 (Figure 9b) and limonene SOA + H_2SO_4 at pH = 2 (Figure 9c). All three spectra were taken under identical instrumental conditions. The intensities in Figure 9a were normalized to the peak corresponding to deprotonated keto-limononic acid ($C_9H_{13}O_4^-$, *m/z 185*.0819), and the same normalization was applied to spectra in Figures 9b and 9c. We intentionally excluded the peak at *m/z* 96.960 corresponding to the HSO_4^- ion, which would have overwhelmed the mass spectrum otherwise, by setting the lower limit for the mass range to *m/z* = 100 during data acquisition. A considerable number of SOC peaks were detected by negative ion mode ESI-MS (Table S2 in the auxiliary material). Tandem mass spectrometry (MS/MS) was performed on prominent SOC peaks to confirm that they represent genuine deprotonated molecular ions, and not weakly bound complexes of the type M—HSO_4^-. The collision energies required to break these ions were characteristic of covalent bonding, and although the collision induced dissociation was dominated by the loss of HSO_4^-, losses of neutral fragments leaving behind ions that retained S-atoms were also observed.

[39] HR MS data can potentially distinguish between reactions (R3) and (R4) because these reactions add an equivalent of SO_3 (79.9568 Da) and H_2SO_4 (97.9674 Da), respectively, to the original molecular formula of the SOC precursor. We examined all SOC compounds observed in the mass spectra, and in most cases each SOC could be matched to either one or both corresponding precursor compounds ($C_cH_hO_oS_s - SO_3$ or $C_cH_hO_oS_s - H_2SO_4$) in the pre-evaporated sample. The results showed no clear pattern that would make it possible to rule out either reaction (R3) or (R4) as possibilities.

[40] The mass spectrum of the evaporated/redissolved SOA solution (Figure 9a) is quite similar to the published ESI mass spectra of limonene SOA extracted in acetonitrile [*Walser et al.*, 2008] or water [*Bateman et al.*, 2010]. The characteristic envelopes corresponding to the monomeric (centered at *m/z* 180) and dimeric (centered at *m/z* 370) compounds are clearly visible in the spectrum. Evaporation/redissolution of SOA + H_2SO_4 at pH = 4 produced a colorless solution and preserved most of the peaks in the original SOA spectrum, including their relative intensity distribution. Several new peaks observed for this system

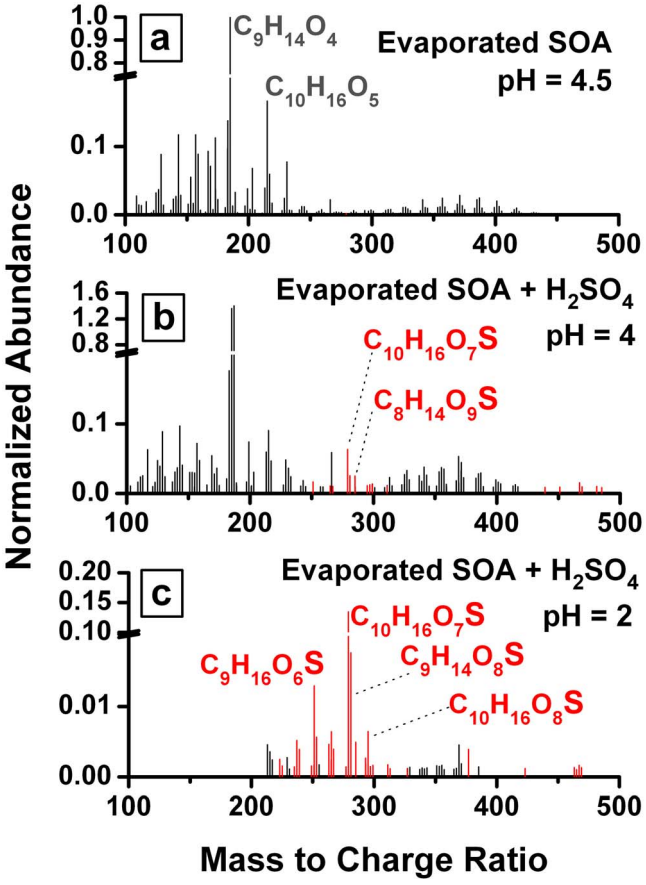

Figure 9. Negative ion mode ESI mass spectra of evaporated/redissolved solutions of: (a) SOA; (b) SOA+ H_2SO_4 at pH = 4; and (c) SOA+ H_2SO_4 at pH = 2. Red peaks correspond to formulas containing sulfur. Assignments of neutral precursors corresponding to selected peaks are shown next to the peaks. All mass spectra were normalized to the intensity of the $C_9H_{13}O_4^-$ peak at *m/z* 185.0819 in the evaporated SOA spectrum. Note the different abundance ranges and breaks in the vertical axis.

Table 1. High-Resolution Mass Spectrometry Results From the Molecular Composition Analysis of Aqueous Extracts of SOA and of SOA Acidified With H_2SO_4 Before and After Evaporation/Redissolution at Different Initial pH Values[a]

Sample	Evaporation	Total Peaks	SOC (% Count)	SOC (% TIC)	⟨O:C⟩
SOA, nothing added	Before	203	0	0	0.50
SOA, nothing added	After	218	0	0	0.48
SOA + H_2SO_4 (pH = 4)	Before	147	7	2	0.51
SOA + H_2SO_4 (pH = 4)	After	138	12	3	0.54
SOA + H_2SO_4 (pH = 2)	Before	95	30	27	0.58
SOA + H_2SO_4 (pH = 2)	After	54	57	85	0.69

[a]Total peaks: the number of assigned peaks below *m/z* 500; % count and % TIC refer to the percentage of the peaks and percentage of the total ion current, respectively, assigned to sulfur-containing organic compounds (SOC). The average O/C ratio is calculated as the intensity-weighted average for all assigned peaks.

correspond to SOC (Figure 9b). Evaporation/redissolution at pH ∼ 2, produced a brown solution, and led to a dramatic change in the appearance of the mass spectrum (Figure 9c). The majority of peaks pertaining to the original SOA material disappeared, and the peaks that remained were dominated by SOC.

[41] Table 1 shows the number of assigned peaks, the fraction of peaks corresponding to SOC, the fractional ion current of SOC, and the intensity-weighted average O/C ratios ($\langle O/C\rangle = \Sigma[o_i \times intensity_i]/\Sigma[c_i \times intensity_i]$) for six types of samples: the pre-evaporated and evaporated/redissolved solutions for each of non-acidified SOA, SOA acidified to pH = 4 and SOA acidified to pH = 2. Evaporation/redissolution of the SOA material without addition of H_2SO_4 did not produce a color change. Furthermore, the average composition of the SOA was not significantly different: 92% of the peaks from the pre-evaporated samples were retained, and the overall number of peaks did not decrease. A small fraction (13% by count) of additional compounds were observed in the non-acidified evaporated SOA sample, suggesting that subtle chemical changes occurred in the evaporation process even without acids present. The new compounds found uniquely in the evaporated sample had an average double bond equivalency (DBE = 1 − h/2 + c) of ⟨DBE⟩ ∼ 5 and ⟨O/C⟩ = 0.38, compared to an average ⟨DBE⟩ ∼ 4 and ⟨O/C⟩ = 0.51 for all the compounds observed in the pre-evaporated sample. This implied that the new compounds formed by the evaporation process on average gained one double bond and lost one oxygen atom. This increase in ⟨DBE⟩ and concurrent decrease in ⟨O/C⟩ is consistent with the production of (colorless) aldol condensation products during evaporation, in which one double bond is added to the molecular structure and one oxygen is removed for each condensation reaction that is accompanied by a loss a water molecule.

[42] In acidified samples, we observe a general trend that the total number of detected peaks decreases, the number of SOC increases, and the ⟨O/C⟩ ratio increases with increasing acidity. Evaporation of the acidified samples further amplifies the trend. The increase in SOC and ⟨O/C⟩ is expected, as reactions (R3) and (R4) produce SOC from H_2SO_4 and enrich the oxygen content of the molecule. The decrease in the total number of peaks is due to the ionization suppression by much more abundant ions HSO_4^- and H_2SO_4-HSO_4^- present in the electrospray. Indeed, the H_2SO_4-HSO_4^- peak would dominate the spectrum in Figure 9c if this peak was not removed as part of the background correction process. At pH = 4, the small amount of added H_2SO_4 resulted in production of 7% assignable peaks corresponding to SOC. Compared to the non-acidified SOA case, the total number of observed peaks decreased from ∼200 to ∼150.

[43] Evaporation/redissolution of the pH = 4 sample increased the ⟨O/C⟩ ratio from 0.51 to 0.54, and increased the fraction of detected SOC, from 7% to 12% by number. At pH = 2, the number of observed peaks in the pre-evaporated sample further decreased to ∼100. The fraction of SOC compounds increased from 7% to 30% and the ⟨O/C⟩ increased from 0.51 to 0.58. Evaporation/redissolution of the pH = 2 sample further increased ⟨O/C⟩ to 0.69, reduced the total number of observed compounds, and dramatically increased the faction of SOC in the sample (∼60% by number). We note that the relative fractions of SOC quoted above should be considered an upper limit because of the high ionization efficiency of SOC in negative ion mode ESI.

[44] In summary, we observed a dramatic change in composition of the acidified and evaporated SOA extracts, which paralleled similarly dramatic changes in the optical and physical (solubility in water) properties of the dissolved organics.

4. Atmospheric Implications

[45] Cloud and fog processing of atmospheric gases and particles is an important driver of atmospheric chemistry. A number of key atmospheric processes occur in water, with the classic example being oxidation of SO_2 to sulfuric acid [*Finlayson-Pitts and Pitts*, 2000]. Organic compounds dissolved in cloud and fog droplets can undergo photooxidation by dissolved OH [*Ervens et al.*, 2008], direct photolysis [*Bateman et al.*, 2011], hydrolysis, and other chemical transformations on atmospherically relevant time scales. However, a number of aqueous phase reactions are too slow under atmospherically relevant conditions because of insufficient reactant concentrations, insufficient time spent by the molecules in droplets, unfavorable equilibria, solubility limitations, etc. Relevant examples include acid-catalyzed aldol condensation of aliphatic carbonyls in aqueous H_2SO_4 [*Casale et al.*, 2007; *Nozière and Esteve*, 2007], formation of organosulfates by esterification of alcohols with H_2SO_4 in aqueous solutions [*Minerath et al.*, 2008], and formation of light-absorbing nitrogen containing compounds in aqueous reactions between SOA compounds and ammonium sulfate (AS) [*Bones et al.*, 2010]. In this work, we demonstrate that evaporation of water droplets, a very common process in the atmosphere, can greatly accelerate some otherwise slow processes, and lead to dramatic changes in the composition or/and optical properties of the dissolved organics. The main driving forces behind this acceleration are increased reactant concentrations and increased acidity produced by evaporation, and in the case of condensation reactions, shifting equlibria toward the products by actively removing water from the system.

[46] More specifically, we have shown that evaporation of solutions containing dissolved SOA material mixed with dissolved AS can produce nitrogen-containing chromophoric compounds. Such compounds represent a minor fraction of

the overall composition, and they would not be readily detectable by online aerosol mass spectrometry methods [*DeCarlo et al.*, 2006; *Noble and Prather*, 2000; *Pratt and Prather*, 2012; *Zahardis et al.*, 2011]. This irreversible process occurs readily over the pH range of 4–9 and requires small amounts of dissolved AS ($\ll$1 mg/L), conditions commonly found in cloud and fog droplets [*Fisak et al.*, 2002; *Gioda et al.*, 2011]. Given the widespread occurrence of SOA and AS in the environment, this evaporation-driven process and similar reactions occurring during evaporation of water from droplets and wet aerosols may be an important pathway to brown carbon. The mass absorption coefficient (*MAC*) for the material produced by evaporations is around 0.1 $m^2\ g^{-1}$ at 500 nm, which is comparable to the measured *MAC* values for the brown carbon obtained by burning wood (<0.5 $m^2\ g^{-1}$ at 500 nm) [*Chen and Bond*, 2010].

[47] In addition, we have shown that evaporation of SOA solutions in the presence of H_2SO_4 produces organosulfates and aldol products. Under sufficiently acidic conditions, at the initial solution pH = 2, evaporation in the presence of H_2SO_4 irreversibly produces light-absorbing products with maximum absorption peaks around 400 nm. High resolution mass spectrometry of the products suggests that this kind of "evaporative processing" results in a dramatic change in the composition of the organics, with a number of the initial compounds being converted into organosulfates and other products. The solubility of the organic material in water is also reduced by this process. Although the acidity of pH = 2 required for these transformations in the composition, solubility, and optical properties is outside the range of relevance for cloud droplets, it can be easily achieved in smaller fog droplets and in hydrated aerosols.

[48] In our experiments, drying the solutions from an equivalent of saturation (RH $\sim$ 100%) to an equivalent of RH $\sim$ 20% triggered a sudden change in the composition and color of the dissolved solutes. Can we expect the conditions in which the RH in the air surrounding droplets or wet aerosols can change from saturated to dry on reasonably fast time scales? Although individual droplets within clouds and fogs appear and evaporate on a time scale of minutes, the interstitial RH remains close to 100% [*Pruppacher and Klett*, 1997] making the evaporation-driven chemistry unlikely. A more likely scenario is evaporation of falling rain droplets before they hit the ground, which is very common in semiarid continental regions and in deserts [*Rosenfeld and Mintz*, 1988]. In these regions falling droplets become exposed to very dry air on their way down, and dry completely, leaving a processed particle behind. Heat-driven dissipation of fogs, which occurs on the time scales of hours, represents another scenario in which evaporation is likely to be important. Transitions between high and low RH conditions should be even more common for aerosols. Although the concentration regime investigated in this work is more relevant for cloud and fog chemistry, especially in polluted urban regions, it is reasonable to assume that the same processes will also occur when internally mixed organic/inorganic aerosols lose adsorbed water by drying. In fact, these evaporation-driven reactions may be even more efficient because of the higher concentrations and, for acid-catalyzed reactions, lower pH values found in wet aerosols.

[49] This work demonstrates that chemical and physical changes may occur in SOA compounds due to atmospheric dynamics. The physical motion of air masses or rain droplets is ultimately responsible for the change in the relative humidity, which then triggers evaporation and the associated chemistry. Therefore, future modeling of the atmospheric significance of these processes, as well as assessing their role in the brown carbon production, will require explicit inclusion of atmospheric dynamics and chromophore formation chemistry in the models.

[50] **Acknowledgments.** The UCI group gratefully acknowledges support by the NSF grants ATM-0831518 and CHE-0909227. The PNNL group acknowledges support provided by the intramural research and development program of the W. R. Wiley Environmental Molecular Sciences Laboratory (EMSL), a national scientific user facility sponsored by the Office of Biological and Environmental Research and located at PNNL. PNNL is operated for the U.S. Department of Energy by Battelle Memorial Institute under contract DE-AC06-76RL0 1830.

References

Barth, M. C. (2006), The importance of cloud drop representation on cloud photochemistry, *Atmos. Res.*, *82*(1–2), 294–309, doi:10.1016/j.atmosres.2005.10.008.

Bateman, A. P., M. L. Walser, Y. Desyaterik, J. Laskin, A. Laskin and S. A. Nizkorodov (2008), The effect of solvent on the analysis of secondary organic aerosol using electrospray ionization mass spectrometry, *Environ. Sci. Technol.*, *42*, 7341–7346., doi:10.1021/es801226w.

Bateman, A. P., S. A. Nizkorodov, J. Laskin, and A. Laskin (2009), Time-resolved molecular characterization of limonene/ozone aerosol using high-resolution electrospray ionization mass spectrometry, *Phys. Chem. Chem. Phys.*, *11*(36), 7931–7942, doi:10.1039/b905288g.

Bateman, A. P., S. A. Nizkorodov, J. Laskin, and A. Laskin (2010), High-resolution electrospray ionization mass spectrometry analysis of water-soluble organic aerosols collected with a particle into liquid sampler, *Anal. Chem.*, *82*(19), 8010–8016, doi:10.1021/ac1014386.

Bateman, A. P., S. A. Nizkorodov, J. Laskin, and A. Laskin (2011), Photolytic processing of secondary organic aerosols dissolved in cloud droplets, *Phys. Chem. Chem. Phys.*, *13*(26), 12,199–12,212, doi:10.1039/c1cp20526a.

Bator, A., and J. L. Collett Jr. (1997), Cloud chemistry varies with drop size, *J. Geophys. Res.*, *102*(D23), 28,071–28,078, doi:10.1029/97JD02306.

Bones, D. L., D. K. Henricksen, S. A. Mang, M. Gonsior, A. P. Bateman, T. B. Nguyen, W. J. Cooper, and S. A. Nizkorodov (2010), Appearance of strong absorbers and fluorophores in limonene-O_3 secondary organic aerosol due to NH_4^+-mediated chemical aging over long time scales, *J. Geophys. Res.*, *115*, D05203, doi:10.1029/2009JD012864.

Capel, P. D., R. Gunde, F. Zuercher, and W. Giger (1990), Carbon speciation and surface tension of fog, *Environ. Sci. Technol.*, *24*(5), 722–727, doi:10.1021/es00075a017.

Carlton, A. G., B. J. Turpin, K. E. Altieri, S. P. Seitzinger, R. Mathur, S. J. Roselle, and R. J. Weber (2008), CMAQ model performance enhanced when in-cloud secondary organic aerosol is included: Comparisons of organic carbon predictions with measurements, *Environ. Sci. Technol.*, *42*(23), 8798–8802, doi:10.1021/es801192n.

Casale, M. T., A. R. Richman, M. J. Elrod, R. M. Garland, M. R. Beaver, and M. A. Tolbert (2007), Kinetics of acid-catalyzed aldol condensation reactions of aliphatic aldehydes, *Atmos. Environ.*, *41*(29), 6212–6224, doi:10.1016/j.atmosenv.2007.04.002.

Chan, M. N., et al. (2010), Characterization and quantification of isoprene-derived epoxydiols in ambient aerosol in the southeastern United States, *Environ. Sci. Technol.*, *44*(12), 4590–4596, doi:10.1021/es100596b.

Chate, D. M., and P. C. S. Devara (2009), Acidity of raindrop by uptake of gases and aerosol pollutants, *Atmos. Environ.*, *43*(8), 1571–1577, doi:10.1016/j.atmosenv.2008.06.031.

Chelf, J. H., and S. T. Martin (1999), Water activity and equilibrium freezing temperatures of aqueous NH_4HSO_4 solutions from −30 to 25°C, *Geophys. Res. Lett.*, *26*(15), 2391–2394, doi:10.1029/1999GL900436.

Chen, Y., and T. C. Bond (2010), Light absorption by organic carbon from wood combustion, *Atmos. Chem. Phys.*, *10*(4), 1773–1787, doi:10.5194/acp-10-1773-2010.

Collett, J. L., A. Bator, D. E. Sherman, K. F. Moore, K. J. Hoag, B. B. Demoz, X. Rao, and J. E. Reilly (2002), The chemical composition of fogs and intercepted clouds in the United States, *Atmos. Res.*, *64*(1-4), 29–40, doi:10.1016/S0169-8095(02)00077-7.

Darer, A. I., N. C. Cole-Filipiak, A. E. O'Connor, and M. J. Elrod (2011), Formation and stability of atmospherically relevant isoprene-derived

organosulfates and organonitrates, *Environ. Sci. Technol.*, *45*(5), 1895–1902, doi:10.1021/es103797z.

DeCarlo, P. F., et al. (2006), Field-deployable, high-resolution, time-of-flight aerosol mass spectrometer, *Anal. Chem.*, *78*(24), 8281–8289, doi:10.1021/ac061249n.

De Haan, D. O., A. L. Corrigan, K. W. Smith, D. R. Stroik, J. J. Turley, F. E. Lee, M. A. Tolbert, J. L. Jimenez, K. E. Córdova, and G. R. Ferrell (2009a), Secondary organic aerosol-forming reactions of glyoxal with amino acids, *Environ. Sci. Technol.*, *43*(8), 2818–2824, doi:10.1021/es803534f.

De Haan, D. O., A. L. Corrigan, M. A. Tolbert, J. L. Jimenez, S. E. Wood, and J. J. Turley (2009b), Secondary organic aerosol formation by self-reactions of methylglyoxal and glyoxal in evaporating droplets, *Environ. Sci. Technol.*, *43*(21), 8184–8190, doi:10.1021/es902152t.

Dziedzic, P., A. Bartoszewicz, and A. Córdova (2009), Inorganic ammonium salts as catalysts for direct aldol reactions in the presence of water, *Tetrahedron Lett.*, *50*(52), 7242–7245, doi:10.1016/j.tetlet.2009.10.014.

Eddingsaas, N. C., D. G. VanderVelde, and P. O. Wennberg (2010), Kinetics and products of the acid-catalyzed ring-opening of atmospherically relevant butyl epoxy alcohols, *J. Phys. Chem. A*, *114*(31), 8106–8113, doi:10.1021/jp103907c.

Engelhart, G. J., A. Asa-Awuku, A. Nenes, and S. N. Pandis (2008), CCN activity and droplet growth kinetics of fresh and aged monoterpene secondary organic aerosol, *Atmos. Chem. Phys.*, *8*(14), 3937–3949, doi:10.5194/acp-8-3937-2008.

Ervens, B., G. Feingold, and S. M. Kreidenweis (2005), Influence of water-soluble organic carbon on cloud drop number concentration, *J. Geophys. Res.*, *110*, D18211, doi:10.1029/2004JD005634.

Ervens, B., A. G. Carlton, B. J. Turpin, K. E. Altieri, S. M. Kreidenweis, and G. Feingold (2008), Secondary organic aerosol yields from cloud-processing of isoprene oxidation products, *Geophys. Res. Lett.*, *35*, L02816, doi:10.1029/2007GL031828.

Esteve, W., and B. Nozière (2005), Uptake and reaction kinetics of acetone, 2-butanone, 2,4-pentanedione, and acetaldehyde in sulfuric acid solutions, *J. Phys. Chem. A*, *109*(48), 10,920–10,928, doi:10.1021/jp051199a.

Facchini, M. C., et al. (1999), Partitioning of the organic aerosol component between fog droplets and interstitial air, *J. Geophys. Res.*, *104*(D21), 26,821–26,832, doi:10.1029/1999JD900349.

Finlayson-Pitts, B. J., and J. N. Pitts (2000), *Chemistry of the Upper and Lower Atmosphere: Theory, Experiments, and Applications*, 1040 pp., Academic, San Diego, Calif.

Fisak, J., M. Tesar, D. Rezacova, V. Elias, V. Weignerova, and D. Fottova (2002), Pollutant concentrations in fog and low cloud water at selected sites of the Czech Republic, *Atmos. Res.*, *64*(1–4), 75–87, doi:10.1016/S0169-8095(02)00081-9.

Galloway, M. M., P. S. Chhabra, A. W. H. Chan, J. D. Surratt, R. C. Flagan, J. H. Seinfeld, and F. N. Keutsch (2009), Glyoxal uptake on ammonium sulphate seed aerosol: Reaction products and reversibility of uptake under dark and irradiated conditions, *Atmos. Chem. Phys.*, *9*(10), 3331–3345, doi:10.5194/acp-9-3331-2009.

Garland, R. M., M. J. Elrod, K. Kincaid, M. R. Beaver, J. L. Jimenez, and M. A. Tolbert (2006), Acid-catalyzed reactions of hexanal on sulfuric acid particles: Identification of reaction products, *Atmos. Environ.*, *40*(35), 6863–6878, doi:10.1016/j.atmosenv.2006.07.009.

Gelencsér, A., A. Hoffer, G. Kiss, E. Tombacz, R. Kurdi, and L. Bencze (2003), In-situ formation of light-absorbing organic matter in cloud water, *J. Atmos. Chem.*, *45*(1), 25–33, doi:10.1023/A:1024060428172.

Geron, C., R. Rasmussen, R. R. Arnts, and A. Guenther (2000), A review and synthesis of monoterpene speciation from forests in the United States, *Atmos. Environ.*, *34*(11), 1761–1781, doi:10.1016/S1352-2310(99)00364-7.

Ghorai, S., A. Laskin, and A. V. Tivanski (2011), Spectroscopic evidence of keto-enol tautomerism in deliquesced malonic acid particles, *J. Phys. Chem. A*, *115*(17), 4373–4380, doi:10.1021/jp112360x.

Gioda, A., G. J. Reyes-Rodríguez, G. Santos-Figueroa, J. L. Collett, Jr., S. Decesari, M. d. C. K. V. Ramos, H. J. C. Bezerra Netto, F. R. de Aquino Neto, and O. L. Mayol-Bracero (2011), Speciation of water-soluble inorganic, organic, and total nitrogen in a background marine environment: Cloud water, rainwater, and aerosol particles, *J. Geophys. Res.*, *116*, D05203, doi:10.1029/2010JD015010.

Gómez-González, Y., et al. (2008), Characterization of organosulfates from the photooxidation of isoprene and unsaturated fatty acids in ambient aerosol using liquid chromatography/(−) electrospray ionization mass spectrometry, *J. Mass Spectrom.*, *43*(3), 371–382, doi:10.1002/jms.1329.

Hallquist, M., et al. (2009), The formation, properties and impact of secondary organic aerosol: Current and emerging issues, *Atmos. Chem. Phys.*, *9*(14/2), 5155–5236, doi:10.5194/acp-9-5155-2009.

Hartz, K. E. H., T. Rosenoeron, S. R. Ferchak, T. M. Raymond, M. Bilde, N. M. Donahue, and S. N. Pandis (2005), Cloud condensation nuclei activation of monoterpene and sesquiterpene secondary organic aerosol, *J. Geophys. Res.*, *110*, D14208, doi:10.1029/2004JD005754.

Hawkins, L. N., L. M. Russell, D. S. Covert, P. K. Quinn, and T. S. Bates (2010), Carboxylic acids, sulfates, and organosulfates in processed continental organic aerosol over the southeast Pacific Ocean during VOCALS-REx 2008, *J. Geophys. Res.*, *115*, D13201, doi:10.1029/2009JD013276.

Hoose, C., U. Lohmann, R. Bennartz, B. Croft, and G. Lesins (2008), Global simulations of aerosol processing in clouds, *Atmos. Chem. Phys.*, *8*(23), 6939–6963, doi:10.5194/acp-8-6939-2008.

Huang, X. H. H., H. S. S. Ip, and J. Z. Yu (2011), Secondary organic aerosol formation from ethylene in the urban atmosphere of Hong Kong: A multiphase chemical modeling study, *J. Geophys. Res.*, *116*, D03206, doi:10.1029/2010JD014121.

Iinuma, Y., C. Mueller, T. Berndt, O. Boege, M. Claeys, and H. Herrmann (2007a), Evidence for the existence of organosulfates from beta-pinene ozonolysis in ambient secondary organic aerosol, *Environ. Sci. Technol.*, *41*(19), 6678–6683, doi:10.1021/es070938t.

Iinuma, Y., C. Mueller, O. Boege, T. Gnauk, and H. Herrmann (2007b), The formation of organic sulfate esters in the limonene ozonolysis secondary organic aerosol (SOA) under acidic conditions, *Atmos. Environ.*, *41*(27), 5571–5583, doi:10.1016/j.atmosenv.2007.03.007.

Iinuma, Y., O. Boege, A. Kahnt, and H. Herrmann (2009), Laboratory chamber studies on the formation of organosulfates from reactive uptake of monoterpene oxides, *Phys. Chem. Chem. Phys.*, *11*(36), 7985–7997, doi:10.1039/b904025k.

Jacob, D. J., J. M. Waldman, J. W. Munger, and M. R. Hoffmann (1984), A field investigation of physical and chemical mechanisms affecting pollutant concentrations in fog droplets, *Tellus, Ser. B*, *36*(4), 272–285, doi:10.1111/j.1600-0889.1984.tb00247.x.

Jaoui, M., E. O. Edney, T. E. Kleindienst, M. Lewandowski, J. H. Offenberg, J. D. Surratt, and J. H. Seinfeld (2008), Formation of secondary organic aerosol from irradiated a-pinene/toluene/NO_x mixtures and the effect of isoprene and sulfur dioxide, *J. Geophys. Res.*, *113*, D09303, doi:10.1029/2007JD009426.

Joos, F., and U. Baltensperger (1991), A field study on chemistry, S(IV) oxidation rates and vertical transport during fog conditions, *Atmos. Environ., Part A*, *25*(2), 217–230, doi:10.1016/0960-1686(91)90292-F.

Kanakidou, M., et al. (2005), Organic aerosol and global climate modelling: A review, *Atmos. Chem. Phys.*, *5*(4), 1053–1123, doi:10.5194/acp-5-1053-2005.

Laskin, J., A. Laskin, P. J. Roach, G. W. Slysz, G. A. Anderson, S. A. Nizkorodov, D. L. Bones, and L. Q. Nguyen (2010), High-resolution desorption electrospray ionization mass spectrometry for chemical characterization of organic aerosols, *Anal. Chem.*, *82*(5), 2048–2058, doi:10.1021/ac902801f.

Liggio, J., and S.-M. Li (2006), Organosulfate formation during the uptake of pinonaldehyde on acidic sulfate aerosols, *Geophys. Res. Lett.*, *33*, L13808, doi:10.1029/2006GL026079.

Limbeck, A., and H. Paxbaum (2000), Dependence of in-cloud scavenging of polar organic aerosol compounds on the water solubility, *J. Geophys. Res.*, *105*(D15), 19,857–19,867, doi:10.1029/2000JD900123.

Lin, B., and W. B. Rossow (1996), Seasonal variation of liquid and ice water path in nonprecipitating clouds over oceans, *J. Clim.*, *9*(11), 2890–2902, doi:10.1175/1520-0442(1996)009<2890:SVOLAI>2.0.CO;2.

Loeffler, K. W., C. A. Koehler, N. M. Paul, and D. O. De Haan (2006), Oligomer formation in evaporating aqueous glyoxal and methyl glyoxal solutions, *Environ. Sci. Technol.*, *40*(20), 6318–6323, doi:10.1021/es060810w.

Maksymiuk, C. S., C. Gayahtri, R. R. Gil, and N. M. Donahue (2009), Secondary organic aerosol formation from multiphase oxidation of limonene by ozone: Mechanistic constraints via two-dimensional heteronuclear NMR spectroscopy, *Phys. Chem. Chem. Phys.*, *11*(36), 7810–7818, doi:10.1039/b820005j.

Mancinelli, V., S. Decesari, M. C. Facchini, S. Fuzzi, and F. Mangani (2005), Partitioning of metals between the aqueous phase and suspended insoluble material in fog droplets, *Ann. Chim.*, *95*(5), 275–290, doi:10.1002/adic.200590033.

Martin, S. T. (2000), Phase transitions of aqueous atmospheric particles, *Chem. Rev.*, *100*(9), 3403–3454, doi:10.1021/cr990034t.

Minerath, E. C., and M. J. Elrod (2009), Assessing the potential for diol and hydroxy sulfate ester formation from the reaction of epoxides in tropospheric aerosols, *Environ. Sci. Technol.*, *43*(5), 1386–1392, doi:10.1021/es8029076.

Minerath, E. C., M. T. Casale, and M. J. Elrod (2008), Kinetics feasibility study of alcohol sulfate esterification reactions in tropospheric aerosols, *Environ. Sci. Technol.*, *42*(12), 4410–4415, doi:10.1021/es8004333.

Nguyen, T. B., P. J. L. Roach, J. Laskin, A. Laskin, and S. A. Nizkorodov (2011), Effect of humidity on the composition of isoprene photooxidation

secondary organic aerosol, *Atmos. Chem. Phys.*, *11*, 6931–6944, doi:10.5194/acp-11-6931-2011.

Nizkorodov, S. A., J. Laskin, and A. Laskin (2011), Molecular chemistry of organic aerosols through the application of high resolution mass spectrometry, *Phys. Chem. Chem. Phys.*, *13*(9), 3612–3629, doi:10.1039/c0cp02032j.

Noble, C. A., and K. A. Prather (2000), Real-time single particle mass spectrometry: A historical review of a quarter century of the chemical analysis of aerosols, *Mass Spectrom. Rev.*, *19*(4), 248–274, doi:10.1002/1098-2787(200007)19:4<248::AID-MAS3>3.0.CO;2-I.

Nozière, B., and W. Esteve (2005), Organic reactions increasing the absorption index of atmospheric sulfuric acid aerosols, *Geophys. Res. Lett.*, *32*, L03812, doi:10.1029/2004GL021942.

Nozière, B., and W. Esteve (2007), Light-absorbing aldol condensation products in acidic aerosols: Spectra, kinetics, and contribution to the absorption index, *Atmos. Environ.*, *41*(6), 1150–1163, doi:10.1016/j.atmosenv.2006.10.001.

Nozière, B., D. Voisin, C. A. Longfellow, H. Friedli, B. E. Henry, and D. R. Hanson (2006), The uptake of methyl vinyl ketone, methacrolein, and 2-methyl-3-butene-2-ol onto sulfuric acid solutions, *J. Phys. Chem. A*, *110*(7), 2387–2395, doi:10.1021/jp0555899.

Nozière, B., P. Dziedzic, and A. Córdova (2007), Formation of secondary light-absorbing "fulvic-like" oligomers: A common process in aqueous and ionic atmospheric particles?, *Geophys. Res. Lett.*, *34*(21), L21812, doi:10.1029/2007GL031300.

Nozière, B., P. Dziedzic, and A. Córdova (2009), Products and kinetics of the liquid-phase reaction of glyoxal catalyzed by ammonium ions (NH_4^+), *J. Phys. Chem. A*, *113*(1), 231–237, doi:10.1021/jp8078293.

Nozière, B., P. Dziedzic, and A. Córdova (2010a), Inorganic ammonium salts and carbonate salts are efficient catalysts for aldol condensation in atmospheric aerosols, *Phys. Chem. Chem. Phys.*, *12*(15), 3864–3872, doi:10.1039/b924443c.

Nozière, B., S. Ekström, T. Alsberg, and S. Holmström (2010b), Radical-initiated formation of organosulfates and surfactants in atmospheric aerosols, *Geophys. Res. Lett.*, *37*, L05806, doi:10.1029/2009GL041683.

Pratt, K. A., and K. A. Prather (2012), Mass spectrometry of atmospheric aerosols—Recent developments and applications. Part II: On-line mass spectrometry techniques, *Mass Spectrom. Rev.*, doi:10.1002/mas.20330, in press.

Pruppacher, H. R., and R. Jaenicke (1995), The processing of water vapor and aerosols by atmospheric clouds, a global estimate, *Atmos. Res.*, *38*(1–4), 283–295, doi:10.1016/0169-8095(94)00098-X.

Pruppacher, H. R., and J. D. Klett (1997), *Microphysics of Clouds and Precipitation*, 2nd ed., 976 pp., Kluwer Acad., Norwell, Mass.

Reemtsma, T., A. These, P. Venkatachari, X. Xia, P. K. Hopke, A. Springer, and M. Linscheid (2006), Identification of fulvic acids and sulfated and nitrated analogues in atmospheric aerosol by electrospray ionization Fourier transform ion cyclotron resonance mass spectrometry, *Anal. Chem.*, *78*(24), 8299–8304, doi:10.1021/ac061320p.

Rincón, A. G., M. I. Guzman, M. R. Hoffmann, and A. J. Colussi (2009), Optical absorptivity versus molecular composition of model organic aerosol matter, *J. Phys. Chem. A*, *113*(39), 10,512–10,520, doi:10.1021/jp904644n.

Rincón, A. G., M. I. Guzman, M. R. Hoffmann, and A. J. Colussi (2010), Thermochromism of model organic aerosol matter, *J. Phys. Chem. Lett.*, *1*(1), 368–373, doi:10.1021/jz900186e.

Rizzi, G. P. (1997), Chemical structure of colored Maillard reaction products, *Food Rev. Int.*, *13*(1), 1–28, doi:10.1080/87559129709541096.

Roach, P. J., J. Laskin, and A. Laskin (2010), Nanospray desorption electrospray ionization: An ambient method for liquid-extraction surface sampling in mass spectrometry, *Analyst*, *135*(9), 2233–2236, doi:10.1039/c0an00312c.

Roesler, E. L., and J. E. Penner (2010), Can global models ignore the chemical composition of aerosols?, *Geophys. Res. Lett.*, *37*, L24809, doi:10.1029/2010GL044282.

Rosenfeld, D., and Y. Mintz (1988), Evaporation of rain falling from convective clouds as derived from radar measurements, *J. Appl. Meteorol.*, *27*, 209–215, doi:10.1175/1520-0450(1988)027<0209:EORFFC>2.0.CO;2.

Sareen, N., A. N. Schwier, E. L. Shapiro, D. Mitroo, and V. F. McNeill (2010), Secondary organic material formed by methylglyoxal in aqueous aerosol mimics, *Atmos. Chem. Phys.*, *10*(3), 997–1016, doi:10.5194/acp-10-997-2010.

Schmitt-Kopplin, P., A. Gelencsér, E. Dabek-Zlotorzynska, G. Kiss, N. Hertkorn, M. Harir, Y. Hong, and I. Gebefugi (2010), Analysis of the unresolved organic fraction in atmospheric aerosols with ultrahigh-resolution mass spectrometry and nuclear magnetic resonance spectroscopy: Organosulfates as photochemical smog constituents, *Anal. Chem.*, *82*(19), 8017–8026, doi:10.1021/ac101444r.

Seinfeld, J. H., and S. N. Pandis (1998), *Atmospheric Chemistry and Physics: From Air Pollution to Climate Change*, 1326 pp., John Wiley, Hoboken, N. J.

Shapiro, E. L., J. Szprengiel, N. Sareen, C. N. Jen, M. R. Giordano, and V. F. McNeill (2009), Light-absorbing secondary organic material formed by glyoxal in aqueous aerosol mimics, *Atmos. Chem. Phys.*, *9*(7), 2289–2300, doi:10.5194/acp-9-2289-2009.

Surratt, J. D., et al. (2007), Evidence for organosulfates in secondary organic aerosol, *Environ. Sci. Technol.*, *41*(2), 517–527, doi:10.1021/es062081q.

Trainic, M., A. Abo Riziq, A. Lavi, J. M. Flores, and Y. Rudich (2011), The optical, physical and chemical properties of the products of glyoxal uptake on ammonium sulfate seed aerosols, *Atmos. Chem. Phys.*, *11*(18), 9697–9707, doi:10.5194/acp-11-9697-2011.

van Reken, T. M., N. L. Ng, R. C. Flagan, and J. H. Seinfeld (2005), Cloud condensation nucleus activation properties of biogenic secondary organic aerosol, *J. Geophys. Res.*, *110*, D07206, doi:10.1029/2004JD005465.

Waldman, J. M., J. W. Munger, D. J. Jacob, R. C. Flagan, J. J. Morgan, and M. R. Hoffmann (1982), Chemical composition of acid fog, *Science*, *218*(4573), 677–680, doi:10.1126/science.218.4573.677.

Walser, M. L., Y. Desyaterik, J. Laskin, A. Laskin, and S. A. Nizkorodov (2008), High-resolution mass spectrometric analysis of secondary organic aerosol produced by ozonation of limonene, *Phys. Chem. Chem. Phys.*, *10*(7), 1009–1022, doi:10.1039/b712620d.

Yu, G., A. R. Bayer, M. M. Galloway, K. J. Korshavn, C. G. Fry, and F. N. Keutsch (2011), Glyoxal in aqueous ammonium sulfate solutions: Products, kinetics and hydration effects, *Environ. Sci. Technol.*, *45*(15), 6336–6342, doi:10.1021/es200989n.

Zahardis, J., S. Geddes, and G. A. Petrucci (2011), Improved understanding of atmospheric organic aerosols via innovations in soft ionization aerosol mass spectrometry, *Anal. Chem.*, *83*(7), 2409–2415, doi:10.1021/ac102737k.

Zhao, J., N. P. Levitt, and R. Zhang (2005), Heterogeneous chemistry of octanal and 2,4-hexadienal with sulfuric acid, *Geophys. Res. Lett.*, *32*, L09802, doi10.1029/2004GL022200.

D. L. Bones, P. B. Lee, S. A. Nizkorodov, T. B. Nguyen, and K. M. Updyke, Department of Chemistry, University of California, Irvine, CA 92697, USA. (nizkorod@uci.edu)

A. Laskin, Environmental Molecular Sciences Laboratory, Pacific Northwest National Laboratory, Richland, WA 99352, USA.

J. Laskin, Chemical and Materials Sciences Division, Pacific Northwest National Laboratory, Richland, WA 99352, USA.